A NOVEL ISOPARAMETRIC FINITE ELEMENT DISPLACEMENT FORMULATION FOR AXISYMMETRIC ANALYSIS OF NEARLY INCOMPRESSIBLE MATERIALS

by

H.S. Yu, G.T. Houlsby and H.J. Burd

Report Number OUEL 1872/91

Soil Mechanics Report Number 114/91

University of Oxford,
Department of Engineering Science,
Parks Road,
Oxford
OX1 3PJ
U.K

Tel. (0865) 273000
Fax. (0865) 273010

A NOVEL ISOPARAMETRIC FINITE ELEMENT DISPLACEMENT FORMULATION FOR AXISYMMETRIC ANALYSIS OF NEARLY INCOMPRESSIBLE MATERIALS

H.S. YU

Department of Civil Engineering and Surveying

University of Newcastle, NSW 2308, Australia

and

G.T. HOULSBY AND H.J. BURD

Department of Engineering Science

University of Oxford, England

SUMMARY

It is well accepted that severe numerical difficulties arise when using the conventional displacement method to analyse incompressible or nearly incompressible solids. These effects are caused by the kinematic constraints imposed on the nodal velocities by the constant volume condition. In elastic-plastic analysis, these effects are due to a conflict between the plastic flow rule and the finite element discretization. Although several methods have been proposed to cope with this problem, none has been based on the appropriate choice of displacement interpolation functions to minimise the constraints. The theoretical formulation of a new six-noded isoparametric displacement finite element, which is well suited for elastic-plastic analysis of axisymmetric constrained solids by using a rational displacement interpolation function, is presented in this paper. The proposed displacement interpolation function implies that the displacement in axial direction and the product of the displacement in radial direction and the radius should be treated as two independent basic variables. Alternatively, the proposed displacement interpolation function can also be implemented in a conventional displacement formulation simply by using a modified shape function matrix. The suitability of the proposed formulations is first studied theoretically by assessing the number of degrees-of-freedom per constraint and then verified by performing numerical experiments on typical boundary value problems which involve incompressible behaviour.

INTRODUCTION

It is well known that in conventional finite element computations using the displacement formulation with elastic-plastic models, numerical solutions often become highly inaccurate in the fully plastic range (*Nagtegaal et al.*[1]; *Sloan*[2]). These effects are caused by the excessive kinematic constraints imposed on the nodal velocities by a conflict between the plastic flow rule and the finite element discretization. The conflict arises when a plastic deformation mode such as the incompressibility condition, as defined by the plastic flow rule, cannot be modelled by the shape functions and the available degrees of freedom for an element.

The consequence of the excessive kinematic constraints is to reduce the number of free degrees-of-freedom in the finite element mesh. Since many of the common elastic-plastic models used in solid mechanics require that incompressibility conditions are satisfied throughout the material in the plastic regime, calculations in which these effects occur have considerable practical importance, and have been the subject of much research.

Depending on the type of calculations performed, the effect of additional constraints may be divided into two categories. Firstly, in a collapse load calculation the effect of incompressibility constraints tends to produce an over-stiff response (*Sloan and Randolph*[3]; *Yu and Houlsby*[4]). Secondly, in a calculation in which the material stresses are of primary importance, the additional imposed constraints often produce spurious oscillations in the stresses across an element (*Naylor*[5]; *Burd and Houlsby*[6]).

A particularly comprehensive analysis of the difficulties associated with finite element calculations in the fully plastic range was given by *Nagtegaal et al.*[1] Having identified the detrimental effect of incompressibility constraints, they proposed a criterion which must be satisfied if the finite element analysis is to yield a satisfactory solution. This criterion, which is based on a limiting mesh consisting of an infinite number of elements of identical type, requires that the number of degrees-of-freedom in an element must be greater than the number of constraints imposed by the incompressibility condition. They further showed that for plane strain problems, only a few of the classical lower order elements are able to meet this requirement, while for axisymmetric problems the situation appeared to be much worse, as none of the common lower order elements would be able to predict collapse loads accurately. To obviate this problem, they proposed an approach in which the volumetric

strain rates and the nodal velocities are admitted as independent variables and different geometric expansions are used for each of these variables. Later this approach was applied to undrained soil mechanics problems by *Toh and Sloan*[7].

As an extension to the analysis for the limiting mesh, *Sloan and Randolph*[3] also analysed the necessary conditions for a mesh consisting of a finite number of elements to be suitable for collapse load calculations. This analysis has shown that the suitability of any finite element mesh is governed by the number of degrees-of-freedom per constraint for an element. When the number of degrees-of-freedom per constraint for an element is greater than unity, most meshes will be suitable for limit load calculations. The reverse is true when the number of degrees-of-freedom per constraint is less than unity. When the number of degrees-of-freedom per constraint is equal to unity, it has been demonstrated that at least half of the boundary degrees-of-freedom must be left unrestrained in order to satisfy the criterion. They have shown that this criterion can be satisfied by the use of higher order elements, since as the order of an element is increased, the number of degrees-of-freedom per element increases faster than the number of incompressibility constraints. According to *Sloan*[2], the lowest order of triangular element for axisymmetric problems suitable for this approach is cubic strain element. Although this approach works well, it suffers from the drawback that the higher order elements cause a large bandwidth in the stiffness matrix, which may require some sophisticated equation solvers.

An alternative approach, which has been widely used to obviate the problems caused by the incompressibility constraints, is the so-called Reduced Integration Method (*Zienkiewicz et al.*[8]; *Malkus and Hughes*[9]). The idea of this approach is to use a limiting number of sampling points in evaluating the element matrices and load vectors. One major effect of this method is to decrease the number of incompressibility constraints on the nodal velocities. This is clearly seen by noting that the maximum number of constraints per element must be less than, or equal to, the total number of integration stations used in forming the element stiffness matrices. A theoretical justification for using Reduced Integration in nearly incompressible displacement formulation has been given by *Malkus and Hughes*[9]. They proved that displacement formulations with Reduced Integration are in certain cases equivalent to mixed formulations(i.e. formulations in which the finite element discretization is based on the use of mixed variable types). This equivalence typically holds in plane strain and three dimensional analysis. However, the equivalence breaks down for the case of axisymmetry. In

addition, it has been shown (*de Borst and Vermeer*[10]) that in problems in which, besides the kinematic constraints of incompressibility, many geometric constraints are present (e.g. deep cone penetration problems with a rough boundary condition on the cone), the Reduced Integration approach may result in inaccurate solutions.

A further effect that can be used to advantage, but has received little attention in the past, is that the number of incompressibility constraints may be reduced by choosing appropriate displacement interpolation functions. A example of this type of approach for one-dimensional problems is given by *Yu and Houlsby*[4].

In this paper, the theoretical criterion originally developed by *Nagtegaal et al.*[1] has been used to assess the suitability of a particular displacement interpolation function when it is to be used together with any constitutive law which attempts to enforce the constant volume condition at failure. After a detailed theoretical study of the influence of the displacement interpolation function on the number of the incompressibility constraints, a novel displacement interpolation function with a six-noded triangular element is found to satisfy the *Nagtegaal* criterion in axisymmetry. Based on the proposed displacement interpolation function and the concept of isoparametric elements, two alternative new displacement finite element formulations are developed.

SUITABILITY OF THE PROPOSED DISPLACEMENT INTERPOLATION FUNCTION

According to the criterion of *Nagtegaal et al*[1], it is necessary to determine the number of degrees-of-freedom per constraint for the limiting case of a very fine mesh in order to ascertain whether a particular element assemblage is suitable for accurate elastic-plastic analysis. The number of degree-of-freedom per constraint is defined as the ratio of degrees of freedom to constraints for an element. A general procedure of determining this ratio for any given element type has been described in detail by *Sloan and Randolph*[3].

Following the same procedure, the conventional six-noded triangular element is used to demonstrate that an analysis of axisymmetric constraint problems is more difficult than that of plane strain problems. It is then shown how the conventional six-noded triangular element can be modified to make it suitable for an elastic-plastic analysis under axisymmetric loadings.

Consider a body, loaded under plane strain or axisymmetric conditions, which is discretized arbitrarily using elements of identical type. The number of degrees-of-freedom per element is:

$$m_e = \frac{1}{\pi} \sum_{i=1}^{n} \theta_i^e \tag{1}$$

where θ_i^e denotes internal angle for node i of element e; n is the number of nodes per element (see Figure 1). Using equation (1), the number of degrees-of-freedom per element can be calculated as $m_e = 4\pi/\pi = 4$ for a six-noded triangular element.

Equation (1) was first derived by *Nagtegaal et al*[1] and thought to be only correct for straight-sided elements. Later *Sloan and Randolph*[3] show that the equation is also true for a grid with curved boundaries provided a relatively fine mesh discretization is used.

Figure 1 shows a conventional six-noded triangular element with straight sides. The displacement increments within each element are usually expressed as:

$$\dot{u} = \dot{r} = c_1 + c_2 r + c_3 z + c_4 r^2 + c_5 rz + c_6 z^2 \tag{2}$$

$$\dot{v} = \dot{z} = c_7 + c_8 r + c_9 z + c_{10} r^2 + c_{11} rz + c_{12} z^2 \tag{3}$$

where $\dot{u}$ and $\dot{v}$ denote velocities in r and z directions respectively; and the $c_1, \ldots, c_{12}$ are unknown coefficients and are functions of nodal velocities and coordinates only.

For plane strain conditions, the incompressibility condition is given by:

$$\frac{\partial \dot{u}}{\partial r} + \frac{\partial \dot{v}}{\partial z} = 0 \tag{4}$$

Differentiating equations (2)-(3) and inserting into the equation (4) results in:

$$(c_2 + c_9) + (2c_4 + c_{11})r + (2c_{12} + c_5)z = 0 \tag{5}$$

In evaluating the element stiffness matrix, the incompressibility condition, represented by equation (5), needs to be satisfied at all Gauss sampling points. For the six-noded triangular element, three and six points Gaussian quadrature is often used for plane strain and axisymmetric loading respectively. This order of numerical integration corresponds to what is commonly denoted by the term 'Full Integration' (*Laursen and Gellert*[11]). In general, the constant volume condition which requires equation (5) to be satisfied at three or more integration points for plane strain finite element calculations only imposes a maximum of three independent constraints on the c_i namely:

$$2c_{12} + c_5 = 2c_4 + c_{11} = c_2 + c_9 = 0 \tag{6}$$

Using equations (1) and (6), it is now possible to ascertain whether the conventional six-noded triangular element is suitable for plane strain elastic-plastic analysis. For this element m_e is equal to four in equation (1) and hence, as the finite element mesh is refined, the number of degree-of-freedom per element tends to approach four. From equation (6) we can see that for plane strain problems the incompressibility condition imposes three independent constraints upon the nodal velocities per element. Therefore, in the limit, the number of degree-of-freedom per constraint is equal to $\frac{4}{3}$, which is greater than unity. Hence the conventional six-noded triangular element is deemed to be generally suitable for plane strain elastic-plastic analysis.

For the case of an axisymmetric analysis, the constant volume condition is given by:

$$\frac{\partial \dot{u}}{\partial r} + \frac{\dot{u}}{r} + \frac{\partial \dot{v}}{\partial z} = 0 \tag{7}$$

Substituting equations (2) and (3) into equation (7) results in the following incompressibility condition:

$$(2c_2 + c_9) + (3c_4 + c_{11})r + (2c_5 + 2c_{12})z + c_1\frac{1}{r} + c_3\frac{z}{r} + c_6\frac{z^2}{r} = 0 \tag{8}$$

If six point integration (conventionally referred to as 'Full Integration') is used then the constant volume condition, represented by equation (8) imposes six independent constraints on nodal velocities:

$$2c_2 + c_9 = 3c_4 + c_{11} = 2c_5 + 2c_{12} = c_1 = c_3 = c_6 = 0 \tag{9}$$

For axisymmetric conditions, equations (1) and (9) reveal that the limiting ratio of degrees-of-freedom to constraints is equal to $\frac{2}{3}$ which is less than unity. As a result, the element is thought to be generally unsuitable for finite element analyses of axisymmetric problems of elastic-plastic deformation.

Comparing the constant volume condition equation (4) for plane strain and equation (7) for axisymmetric conditions, it may be seen that the three additional constraints imposed in the axisymmetric formulation are caused by the additional hoop strain term. These additional constraints may be removed if the formulation is based on the generalized radial coordinate R and its velocities $\dot{R}$ which satisfy the following condition:

$$\frac{\partial \dot{R}}{\partial R} = \frac{\partial \dot{u}}{\partial r} + \frac{\dot{u}}{r} = \frac{\partial \dot{r}}{\partial r} + \frac{\dot{r}}{r} \tag{10}$$

The incompressibility condition, equation (7), for axisymmetric cases may now be cast in the same form as the incompressibility condition equation (4) for plane strain:

$$\frac{\partial \dot{R}}{\partial R} + \frac{\partial \dot{z}}{\partial z} = 0 \tag{11}$$

If the formulation is based on the use of a quadratic expansion for the velocities, then:

$$\dot{R} = c_1 + c_2 R + c_3 z + c_4 R^2 + c_5 Rz + c_6 z^2 \tag{12}$$

$$\dot{z} = c_7 + c_8 R + c_9 z + c_{10} R^2 + c_{11} Rz + c_{12} z^2 \tag{13}$$

If equations (12) and (13) are substituted into equation (11) then it may be easily shown that the number of incompressibility constraints is three, rather than the six that are obtained using the conventional displacement formulation. Equation (10) can be solved to give solutions for R and $\dot{R}$ as follows:

$$R = r^2 \tag{14}$$

$$\dot{R} = 2\dot{r}r = 2\dot{u}r \tag{15}$$

In conclusion, the above analysis suggests that under plane strain conditions, the conventional six-noded triangular element can be used to furnish accurate solutions for elastic-plastic analysis, provided it is used in a mesh which is fine enough as this element provides more degrees of freedom than the constraints imposed by incompressibility condition. However, for axisymmetric loading the conventional six-noded triangular element fails to satisfy the criterion of *Nagtegaal et al*, and is unsuitable for elastic-plastic analysis. It has been shown that the six-noded triangular with the modified displacement interpolation function, as defined by equations (12)-(15), can be used to meet the requirement that the limiting number of degrees-of-freedom per constraint must exceed unity in axisymmetric conditions.

The analysis presented so far is limited to the use of straight-sided six-noded triangles for finite element calculations based on any constitutive model which enforces the constant volume condition. However, it is evident that similar problems of over-constraint caused by constant dilation rate conditions will arise when using the conventional displacement formulations together with frictional-dilational plasticity models. The arguments for determining the suitability of an element for nearly incompressibility analysis may also be adopted to assess the suitability of an element for dilational materials (e.g. *Sloan*[2]).

Although the assumption of straight-sided triangular elements is reasonable for many problems, it is not true in some cases (e.g. large displacement analysis). It is therefore neccessary to study effect of curved-sided triangular elements on the analysis for the suitability of straight-sided elements presented in this section. The detailed discussion of this effect will be given in a later section.

FINITE ELEMENT FORMULATION BASED ON MODIFIED PRIMARY VARIABLES

The new velocity expansion function, as defined by equations (12)-(15), has been proved to be suitable for general elastic-plastic analysis under axisymmetric conditions. Based on this expansion, two alternative approaches may be used to form an isoparametric finite element displacement formulation. Firstly, in order to implement the new velocity expansion, we can adopt the velocity of the generalized radial coordinate, $\dot{R}$, as an independent variable and the conventional axial velocity $\dot{z}$ as another basic variable. Then application of the principle of virtual dispalcement to an element in the original coordinates (r, z) may be expressed purely in terms of the variables defined in the generalized coordinates (R, z). It should be noted that the new formulation based on the generalised coordinates is valid for elements of an arbitrary order but it is illustrated with reference to the six-noded triangle in this paper. As a result, a finite element formulation based on the generalized coordinates (R, z) can be formed simply by applying the principle of virtual displacement. In the second approach, the primary variables $[\dot{u}, \dot{v}]^T$ are left unchanged but modifications are made to the element shape functions.

This section is devoted to a description of the first of these two approaches.

The Strain Rate - Velocity Relationship

Figure 2 shows an isoparametric six-noded triangular element e plotted in the original cordinates (r, z), the generalized coordinates (R, z) and the area coordinates (α, β) which corresponds to the element e in the generalized coordinates.

The velocity field vector, $\mathbf{u_m}$, is defined :

$$\mathbf{u_m} = [\dot{R}, \dot{z}]^T = [2\dot{u}r, \dot{v}]^T \tag{16}$$

the strain rate vector may be written in terms of the velocity vector :

$$\dot{\epsilon} = [\dot{\epsilon_r}, \dot{\epsilon_z}, \dot{\epsilon_\theta}, \dot{\gamma_{rz}}]^T = \mathbf{L}\mathbf{u_m} \tag{17}$$

where the linear operator matrix $\mathbf{L}$ is defined:

$$\mathbf{L} = \begin{bmatrix} \frac{\partial}{\partial R} - \frac{1}{2R} & 0 \\ 0 & \frac{\partial}{\partial z} \\ \frac{1}{2R} & 0 \\ \frac{1}{2\sqrt{R}}\frac{\partial}{\partial z} & 2\sqrt{R}\frac{\partial}{\partial R} \end{bmatrix} \tag{18}$$

The Strain Rate - Nodal Velocity Matrices

The nodal velocity vector, $\mathbf{a_m^e}$, is defined :

$$\mathbf{a_m^e} = [2\dot{u_1}r_1, \dot{v_1} \ldots 2\dot{u_6}r_6, \dot{v_6}]^T \tag{19}$$

The nodal velocity vector is related to the velocity field vector by :

$$\mathbf{u_m} = \mathbf{N}\mathbf{a_m^e} \tag{20}$$

where $\mathbf{N}$, the shape function matrix contains the conventional quadratic shape functions written in the area coordinates:

$$\mathbf{N} = \begin{bmatrix} N_1 & 0 & N_2 & 0 & \ldots & N_6 & 0 \\ 0 & N_1 & 0 & N_2 & \ldots & 0 & N_6 \end{bmatrix} \tag{21}$$

where,

$$N_1 = 2(\alpha + \beta - 1)(\alpha + \beta - \frac{1}{2}) \tag{22}$$

$$N_2 = 2\alpha(\alpha - \frac{1}{2}) \tag{23}$$

$$N_3 = 2\beta(\beta - \frac{1}{2}) \tag{24}$$

$$N_4 = -4\alpha(\alpha + \beta - 1) \tag{25}$$

$$N_5 = 4\alpha\beta \tag{26}$$

$$N_6 = -4\beta(\alpha + \beta - 1) \tag{27}$$

The strain rate vector is given by:

$$\dot{\epsilon} = \mathbf{L}\mathbf{u}_\mathbf{m} = \mathbf{L}\mathbf{N}\mathbf{a}^\mathbf{e}_\mathbf{m} = \mathbf{B}\mathbf{a}^\mathbf{e}_\mathbf{m} \tag{28}$$

where

$$\mathbf{B} = \mathbf{L}\mathbf{N} = \begin{bmatrix} \frac{\partial N_1}{\partial R} - \frac{N_1}{2R} & 0 & \dots & \frac{\partial N_6}{\partial R} - \frac{N_6}{2R} & 0 \\ 0 & \frac{\partial N_1}{\partial z} & \dots & 0 & \frac{\partial N_6}{\partial z} \\ \frac{N_1}{2R} & 0 & \dots & \frac{N_6}{2R} & 0 \\ \frac{\partial N_1}{2\sqrt{R}\partial z} & 2\sqrt{R}\frac{\partial N_1}{\partial R} & \dots & \frac{\partial N_6}{2\sqrt{R}\partial z} & 2\sqrt{R}\frac{\partial N_6}{\partial R} \end{bmatrix} \tag{29}$$

The Nodal Force - Nodal Velocity Relationship

The application of the principle of virtual displacement to an element in the original coordinates (r, z) can be used to give the following nodal force - nodal velocity relationship, which may be expressed in terms the variables in the generalized coordinates (R, z) as follows:

$$\dot{\mathbf{P}}^\mathbf{e}_\mathbf{m} = \pi \int \int_{V^e} \mathbf{B}^\mathbf{T} \dot{\sigma} dR dz = \mathbf{K}\mathbf{a}^\mathbf{e}_\mathbf{m} \tag{30}$$

where,

$$\dot{\mathbf{P}}^\mathbf{e}_\mathbf{m} = [(\pi p_h)_1, (2\pi r p_v)_1 ... (\pi p_h)_6, (2\pi r p_v)_6]^T \tag{31}$$

in which p_h and p_v are nodal force increments per unit length in radial and axial directions respectively; The element stiffness matrix $\mathbf{K}$ is defined as:

$$\mathbf{K} = \pi \int \int_{(\alpha,\beta)} \mathbf{B}^\mathbf{T} \mathbf{D}^\mathbf{ep} \mathbf{B} det J d\alpha d\beta \tag{32}$$

where the elastic-plastic stress-strain matrix $\mathbf{D}^\mathbf{ep}$ is defined by:

$$\dot{\sigma} = \mathbf{D}^{\mathbf{ep}}\dot{\epsilon} \tag{33}$$

and the stress vector

$$\sigma = [\sigma_r, \sigma_z, \sigma_\theta, \tau_{rz}]^T \tag{34}$$

is defined graphically in Figure 3 for axisymmetric problems.

The Jacobian determinant $detJ$ in equation (32) is defined by:

$$detJ = \begin{vmatrix} \frac{\partial R}{\partial \alpha} & \frac{\partial R}{\partial \beta} \\ \frac{\partial z}{\partial \alpha} & \frac{\partial z}{\partial \beta} \end{vmatrix} \tag{35}$$

For isoparametric formulations, the coordinate and velocity polynomial expansions are of the same order, namely:

$$R = \sum N_j R_j \tag{36}$$

$$z = \sum N_j z_j \tag{37}$$

where (R_j, z_j) denotes generalised coordinates of node j.

By using the above equations, the Jacobian determinant may be determined by:

$$detJ = \begin{vmatrix} \sum \frac{\partial N_j}{\partial \alpha} R_j & \sum \frac{\partial N_j}{\partial \beta} R_j \\ \sum \frac{\partial N_j}{\partial \alpha} z_j & \sum \frac{\partial N_j}{\partial \beta} z_j \end{vmatrix} \tag{38}$$

Once the Jacobian deterimiant is computed, the derivatives defined in the **B** matrix may be determined as follows:

$$\frac{\partial N_i}{\partial R} = \begin{vmatrix} \frac{\partial N_i}{\partial \alpha} & \frac{\partial z}{\partial \alpha} \\ \frac{\partial N_i}{\partial \beta} & \frac{\partial z}{\partial \beta} \end{vmatrix} / detJ \tag{39}$$

$$\frac{\partial N_i}{\partial z} = \begin{vmatrix} \frac{\partial R}{\partial \alpha} & \frac{\partial N_i}{\partial \alpha} \\ \frac{\partial R}{\partial \beta} & \frac{\partial N_i}{\partial \beta} \end{vmatrix} / detJ \tag{40}$$

The Nodal Force Vectors

Expressions are now given for each of three types of nodal force vectors for axisymmetric elastic-plastic analyses performed with the new six-noded triangular element.

Residual Stresses

The element nodal force vector as a result of residual stresses σ_0 is determined in the following manner beginning with equation (30):

$$\mathbf{P}^{\mathbf{e}}_{\mathbf{m}\sigma_\mathbf{0}} = \pi \int \int_{(\alpha,\beta)} B^T \sigma_0 det J d\alpha d\beta \tag{41}$$

Body Forces

The body forces per unit volume in the radial and axial directions are defined as b_r and b_z respectively. The corresponding nodal force vector is evaluated by appling the virtual work principle to an element in the oringinal coordinates,

$$\mathbf{P}^{\mathbf{e}}_{\mathbf{mb}} = \pi \int \int_{(\alpha,\beta)} \mathbf{N}^{\mathbf{T}}_{\mathbf{m}} \mathbf{b} det J d\alpha d\beta \tag{42}$$

where

$$\mathbf{N_m} = \begin{bmatrix} \frac{N_1}{2r} & 0 & \dots & \frac{N_6}{2r} & 0 \\ 0 & N_1 & \dots & 0 & N_6 \end{bmatrix} \tag{43}$$

and

$$\mathbf{b} = [b_r, b_z]^T \tag{44}$$

Surface Tractions

The integral representing the nodal force vector as a result of the surface tractions is not a volume integral, but rather a surface integral.

Figure 4 shows a distributed pressure defined by two components q and p acting on one of the edges of an element. For an infinitesimal section along the loaded boundary, dl, inclined at an angle θ to the positive r direction, the applied surface pressures can be resolved into two surface tractions s_r and s_z which are in the direction of the coordinate axes r and z,

$$s_r dl = q dl \cos\theta - p dl \sin\theta \tag{45}$$

$$s_z dl = q dl \sin\theta + p dl \cos\theta \tag{46}$$

The above equations may also be written in terms of the generalized coordinates R and z by:

$$\begin{bmatrix} s_r \\ s_z \end{bmatrix} dl = \begin{bmatrix} \frac{q}{2r} dR - p dz \\ q dz + \frac{p}{2r} dR \end{bmatrix} \tag{47}$$

By using the virtual work principle, the equivalent nodal force vector can be shown to be:

$$\mathbf{P}^{\mathbf{e}}_{\mathbf{ms}} = \pi \int_{\xi} \mathbf{N}^{\mathbf{T}}_{\mathbf{mm}} \begin{bmatrix} \frac{q}{2r}\frac{\partial R}{\partial \xi} - p\frac{\partial z}{\partial \xi} \\ q\frac{\partial z}{\partial \xi} + \frac{p}{2r}\frac{\partial R}{\partial \xi} \end{bmatrix} d\xi \tag{48}$$

where

$$\mathbf{N}_{\mathbf{mm}} = \begin{bmatrix} N_1 & 0 & N_2 & 0 & N_4 & 0 \\ 0 & 2N_1 r & 0 & 2N_2 r & 0 & 2N_4 r \end{bmatrix} \tag{49}$$

in which $\alpha = \frac{1}{2}(\xi + 1)$

FINITE ELEMENT FORMULATION BASED ON MODIFIED SHAPE FUNCTIONS

An alternative procedure for implementing a finite element formulation based on the velocity expansions given in equations (12) and (13) is described in this section. In this approach, the conventional primary variables are retained but modifications are made to the shape functions.

The Strain Rate - Velocity Relationship

The velocity field vector $\mathbf{u}$ is defined in the conventional way:

$$\mathbf{u} = [\dot{r}, \dot{z}]^T = [\dot{u}, \dot{v}]^T \tag{50}$$

The strain rate vector is written in terms of the velocity vector:

$$\dot{\epsilon} = [\dot{\epsilon_r}, \dot{\epsilon_z}, \dot{\epsilon_\theta}, \dot{\gamma_{rz}}]^T = \mathbf{L_n u} \tag{51}$$

where the linear operator matrix $\mathbf{L_n}$ is

$$\mathbf{L_n} = \begin{bmatrix} \frac{\partial}{\partial r} & 0 \\ 0 & \frac{\partial}{\partial z} \\ \frac{1}{r} & 0 \\ \frac{\partial}{\partial z} & \frac{\partial}{\partial r} \end{bmatrix} \tag{52}$$

The Strain Rate - Nodal Velocity Matrices

In this approach, the conventional nodal velocity vector $\mathbf{a^e}$ is used:

$$\mathbf{a^e} = [\dot{u_1}, \dot{v_1}, \ldots, \dot{u_6}, \dot{v_6}]^T \tag{53}$$

The proposed velocity expansion function defined by equations (12)-(15) is used to relate the velocity field vector $\mathbf{u}$ to nodal velocity vector $\mathbf{a^e}$ as follows:

$$\mathbf{u} = \mathbf{N_n a^e} \tag{54}$$

where the new shape function matrix $\mathbf{N_n}$ is defined:

$$\mathbf{N_n} = \begin{bmatrix} \bar{N}_1 & 0 & \dots & \bar{N}_6 & 0 \\ 0 & N_1 & \dots & 0 & N_6 \end{bmatrix} \tag{55}$$

and

$$\bar{N}_i = \frac{N_i r_i}{r} \tag{56}$$

in which the functions $N_1, N_2, \dots, N_6$ are given by equations (22)-(27).

Substituting equation (54) into (51) results in:

$$\dot{\epsilon} = \mathbf{L_n u} = \mathbf{L_n N_n a^e} = \mathbf{B_n a^e} \tag{57}$$

where

$$\mathbf{B_n} = \mathbf{L_n N_n} = \begin{bmatrix} \frac{\partial \bar{N}_1}{\partial r} & 0 & \dots & \frac{\partial \bar{N}_6}{\partial r} & 0 \\ 0 & \frac{\partial N_1}{\partial z} & \dots & 0 & \frac{\partial N_6}{\partial z} \\ \frac{\bar{N}_1}{r} & 0 & \dots & \frac{\bar{N}_6}{r} & 0 \\ \frac{\partial \bar{N}_1}{\partial z} & \frac{\partial N_1}{\partial r} & \dots & \frac{\partial \bar{N}_6}{\partial z} & \frac{\partial N_6}{\partial r} \end{bmatrix} \tag{58}$$

and

$$\frac{\partial \bar{N}_i}{\partial r} = -r_i \frac{N_i}{R} + 2r \frac{\partial N_i}{\partial R} \tag{59}$$

$$\frac{\bar{N}_i}{r} = r_i \frac{N_i}{R} \tag{60}$$

$$\frac{\partial \bar{N}_i}{\partial z} = \frac{r_i}{r} \frac{\partial N_i}{\partial z} \tag{61}$$

in which $\frac{\partial N_i}{\partial R}$ and $\frac{\partial N_i}{\partial z}$ are defined by equations (39)-(40).

The Nodal Force - Nodal Velocity Relationship

The virtual work principle can be used to give the following nodal force - nodal velocity relationship:

$$\dot{\mathbf{P}}^{\mathbf{e}} = \pi \int \int_{V^e} \mathbf{B_n} \dot{\sigma} dR dz = \mathbf{K_n a^e} \tag{62}$$

where the nodal force vector is defined by:

$$\dot{\mathbf{P}}^{\mathbf{e}} = [(2\pi r p_h)_1, (2\pi r p_v)_1 ... (2\pi r p_h)_6, (2\pi r p_v)_6]^T \tag{63}$$

in which p_h and p_v represent nodal force increments per unit length in radial and axial directions respectively; The element stiffness matrix $\mathbf{K_n}$ is defined as :

$$\mathbf{K_n} = \pi \int \int_{(\alpha,\beta)} \mathbf{B_n^T D^{ep} B_n} det J d\alpha d\beta \tag{64}$$

and the elastic-plastic stress-strain matrix $\mathbf{D^{ep}}$ and the Jacobian determiant $detJ$ are the same as defined by equations (32) and (38) in the previous section.

The Nodal Force Vectors

In contrast to the formulation presented in the previous section, different velocity vectors and nodal force vectors are used in this section. Hence, it is neccessary to derive expressions of the nodal force vectors caused by certain loadings.

Residual Stresses

By using the equation (62), we may write the element nodal force vector as a result of residual stresses σ_0 as follows:

$$\mathbf{P^e_{\sigma_0}} = \pi \int \int_{(\alpha,\beta)} \mathbf{B_n^T} \sigma_0 det J d\alpha d\beta \tag{65}$$

Body Force

The application of virtual work principle to an element may be used to give:

$$\mathbf{P^e_b} = \pi \int \int_{(\alpha,\beta)} \mathbf{N_n^T b} det J d\alpha d\beta \tag{66}$$

where the body force vector $\mathbf{b}$ is defined by equation (44).

Surface Tractions

Applying the virtual displacement principle to an element shown in Figure 4, the equivalent nodal force vector may be shown to be:

$$\mathbf{P}_{\mathbf{s}}^{\mathbf{e}} = 2\pi \int_{\xi} \mathbf{N}_{\mathbf{n}}^{\mathbf{T}} r \begin{bmatrix} \frac{q}{2r}\frac{\partial R}{\partial \xi} - p\frac{\partial z}{\partial \xi} \\ q\frac{\partial z}{\partial \xi} + \frac{p}{2r}\frac{\partial R}{\partial \xi} \end{bmatrix} d\xi \tag{67}$$

where

$$\mathbf{N_n} = \begin{bmatrix} \bar{N}_1 & 0 & \bar{N}_2 & 0 & \bar{N}_4 & 0 \\ 0 & N_1 & 0 & N_2 & 0 & N_4 \end{bmatrix} \tag{68}$$

in which $\alpha = \frac{1}{2}(\xi + 1)$.

FINITE ELEMENT DISCRETIZATION AND EFFECTS OF ELEMENT SHAPE

The two key ideas of the finite element method are (1) discretization of the region into finite elements and (2) the use of interpolating polynomials to describe the variation of a field variable within an element. The development of a rational displacement interpolation function has been discussed in the preceding section.

As far as discretization is considered, there are two ways by which finite element formulations using the new six-noded triangular element described in this paper may be implemented. First of all, the region being analysed defined in the original coordinates (r, z) can be discretized into many six-noded triangular elements and then these triangles should be mapped into the generalized coordinates (R, z) element by element. Alternatively, we can first map the whole region from the original coordinates into the generalized coordinates and then generate an element mesh in the region being analysed in the generalized coordinates. Because of the mapping, the use of the first approach produces triangular elements with curved sides in the generalized coordinates, whilst the second approach may generate straight-sided triangles in the generalized coordinates, corresponding to curved-sided elements in the original coordinates. As the element stiffness matrix, as defined by equation (32) or (60), should be calculated using an element geometry defined in the generalized coordinates (R, z), the second approach, which produces straight-sided elements in

the generalized coordinates, is preferable. The second approach is also more convenient to implement with a mesh generator.

In previous sections, the suitability of the new six-noded triangular element was assessed by assuming that all triangles had straight sides. Although this assumption is satisfactory for many problems, it is neccessary to employ elements with irregular shapes in some cases (e.g. the first approach to discretization; or the second approach of discretization for a large displacement analysis). In order to assess the effect of element shapes used for calculations, the suitability of the new six-noded triangular element with curved sides used in elastic-plasic analyses under axisymmetric conditions is now investigated.

For a mesh of six-noded triangles for which the sides are not necessarily straight, the generalized area coordinates (α, β) are no longer coincident with the global coordinates (R, z). Use of the proposed velocity expansion function (equation (12)-(15)) may be made to give the velocity at any point within an element in the following form:

$$\dot{R} = \bar{b_1} + \bar{b_2}\alpha + \bar{b_3}\beta + \bar{b_4}\alpha^2 + \bar{b_5}\alpha\beta + \bar{b_6}\beta^2 \tag{69}$$

$$\dot{z} = \bar{b_7} + \bar{b_8}\alpha + \bar{b_9}\beta + \bar{b_{10}}\alpha^2 + \bar{b_{11}}\alpha\beta + \bar{b_{12}}\beta^2 \tag{70}$$

using the chain rule:

$$\frac{\partial \dot{R}}{\partial R} = \frac{\partial \dot{R}}{\partial \alpha}\frac{\partial \alpha}{\partial R} + \frac{\partial \dot{R}}{\partial \beta}\frac{\partial \beta}{\partial R} \tag{71}$$

and

$$\frac{\partial \dot{z}}{\partial z} = \frac{\partial \dot{z}}{\partial \alpha}\frac{\partial \alpha}{\partial z} + \frac{\partial \dot{z}}{\partial \beta}\frac{\partial \beta}{\partial z} \tag{72}$$

Differentiating equations (69) and (70), inserting in equations (71) and (72), and utilizing the axisymmetric incompressibility condition defined by equation (11) results in:

$$\begin{aligned} (\bar{b_2} + 2\bar{b_4}\alpha + \bar{b_5}\beta)\frac{\partial \alpha}{\partial R} + (\bar{b_3} + \bar{b_5}\alpha + 2\bar{b_6}\beta)\frac{\partial \beta}{\partial R} \quad + \\ (\bar{b_8} + 2\bar{b_{10}}\alpha + \bar{b_{11}}\beta)\frac{\partial \alpha}{\partial z} + (\bar{b_9} + \bar{b_{11}}\alpha + 2\bar{b_{12}}\beta)\frac{\partial \beta}{\partial z} \quad = \quad 0 \end{aligned} \tag{73}$$

By using the definition of the Jacobian, we have:

$$\begin{bmatrix} \frac{\partial\alpha}{\partial R} & \frac{\partial\alpha}{\partial z} \\ \frac{\partial\beta}{\partial R} & \frac{\partial\beta}{\partial z} \end{bmatrix} = \frac{1}{detJ} \begin{bmatrix} \frac{\partial z}{\partial\beta} & -\frac{\partial R}{\partial\beta} \\ -\frac{\partial z}{\partial\alpha} & \frac{\partial R}{\partial\alpha} \end{bmatrix} \tag{74}$$

where Jacobian determinant $detJ$ is defined by equation (35).

Substituting the above equation into equation (73) furnishes:

$$\begin{aligned} (\bar{b_2} + 2\bar{b_4}\alpha + \bar{b_5}\beta)\frac{\partial z}{\partial\beta} - (\bar{b_3} + \bar{b_5}\alpha + 2\bar{b_6}\beta)\frac{\partial z}{\partial\alpha} \quad - \\ (\bar{b_8} + 2\bar{b_{10}}\alpha + \bar{b_{11}}\beta)\frac{\partial R}{\partial\beta} + (\bar{b_9} + \bar{b_{11}}\alpha + 2\bar{b_{12}}\beta)\frac{\partial R}{\partial\alpha} \quad = \quad 0 \end{aligned} \tag{75}$$

For isoparametric formulations, the geometry expansion and velocity expansion are of the same order. The location of any point with a six-noded triangular element is thus defined by:

$$R = b_1 + b_2\alpha + b_3\beta + b_4\alpha^2 + b_5\alpha\beta + b_6\beta^2 \tag{76}$$

$$z = b_7 + b_8\alpha + b_9\beta + b_{10}\alpha^2 + b_{11}\alpha\beta + b_{12}\beta^2 \tag{77}$$

where $b_1, b_2, \ldots, b_{12}$ are functions of generalized nodal coordinates only.

Differentiating equations (76) and (77) and inserting equation (75) gives the following incompressibility condition:

$$\bar{c_1} + \bar{c_2}\alpha + \bar{c_3}\beta + \bar{c_4}\alpha^2 + \bar{c_5}\alpha\beta + \bar{c_6}\beta^2 = 0 \tag{78}$$

where

$$\bar{c_1} = \bar{b_2}b_9 - \bar{b_3}b_8 - \bar{b_8}b_3 + \bar{b_9}b_2 \tag{79}$$

$$\bar{c_2} = \bar{b}2b_{11} + 2\bar{b_4}b_9 - 2\bar{b_3}b_{10} - \bar{b_5}b_{11} - \bar{b_8}b_5 - 2\bar{b_{10}}b_3 + 2\bar{b_{10}}b_4 + \bar{b_{11}}b_2 \tag{80}$$

$$\bar{c_3} = \bar{b_5}b_9 + 2\bar{b_2}b_{12} - \bar{b_3}b_{11} - 2\bar{b_6}b_8 - 2\bar{b_8}b_{10} - \bar{b_{11}}b_3 + \bar{b_9}b_5 + 2\bar{b_{12}}b_2 \tag{81}$$

$$\bar{c_4} = 2\bar{b_4}b_{11} - 2\bar{b_5}b_{10} - 2\bar{b_{10}}b_5 + 2\bar{b_{11}}b_4 \tag{82}$$

$$\bar{c_5} = 4\bar{b_4}b_{11} - 4\bar{b_6}b_{10} - 4\bar{b_{10}}b_6 + 4\bar{b_{12}}b_4 \tag{83}$$

$$\bar{c_6} = 2\bar{b_5}b_{12} - 2\bar{b_6}b_{11} - 2\bar{b_{11}}b_6 + 2\bar{b_{12}}b_5 \tag{84}$$

Before we can assess the number of the constraints imposed by the incompressibility condition equation (78) on nodal velocities, the appropriate order of quadrature for the new six-noded triangular element used for axisymmetric problems needs to be discussed. The best order of quadrature is usually decided after numerical testing, since the profits and pitfalls of a particular rule are hard to forsee. Often it is best to use as low an order as possible without numerical error because fewer points rule results in lower computation cost.

There is a lower limit on the number of sampling points because the quadrature rule must be sufficient to integrate the element volume exactly. The argument begins with the observation that as a mesh is refined and a constant strain condition prevails in each element, which implies a constant strain energy density for elastic materials, the strain energy for an elastic structure is correctly assessed if the volume of the structure is correctly computed. For the new six-noded triangular element of finite size used for axisymmetric problems, we need to find a rule which can integrate the element volume, as defined by:

$$V^e = 2\pi \int\int_{(r,z)} r dr dz = \pi \int\int_{(R,z)} dR dz = \pi \int\int_{(\alpha,\beta)} detJ d\alpha\beta \tag{85}$$

correctly. From equations (38) and (21)-(26) we may note that the Jacobian determinant $detJ$ contains α^2 and β^2, so a three-point rule is needed. It can easily be proved that for the conventional six-noded triangular element used for plane strain problems a three-point integration rule is needed to assess the element volume correctly.

For conventional six-noded triangular elements used for axisymmetric configurations, the element volume may be defined in the form:

$$\bar{V}^e = 2\pi \int\int_{(r,z)} r dr dz = 2\pi \int\int_{(\bar{\alpha},\bar{\beta})} r det\bar{J} d\bar{\alpha} d\bar{\beta} \tag{86}$$

note here $\bar{\alpha}, \bar{\beta}$ denote the conventional area coordinates of the element defined in the coordinates (r, z). For an isoparametric element, $r det\bar{J}$ may be proved to contain $\bar{\alpha}^4$ and $\bar{\beta}^4$, so a six-point rule is needed to assess the element volume correctly. This order of the quadrature rule corresponds to the so-called 'Full-Integration'.

If a three-point rule is used, the incompressibility condition, represented by equation (78), needs to be satisfied at three independent locations within the element. Adopting matrix notation, the constant volume requirement may be written in the matrix form:

$$\begin{bmatrix} 1 & \alpha_1 & \beta_1 & \alpha_1^2 & \alpha_1\beta_1 & \beta_1^2 \\ 1 & \alpha_2 & \beta_2 & \alpha_2^2 & \alpha_2\beta_2 & \beta_2^2 \\ 1 & \alpha_3 & \beta_3 & \alpha_3^2 & \alpha_3\beta_3 & \beta_3^3 \end{bmatrix} \begin{pmatrix} \bar{c_1} \\ \bar{c_2} \\ \bar{c_3} \\ \bar{c_4} \\ \bar{c_5} \\ \bar{c_6} \end{pmatrix} = 0 \tag{87}$$

in general, the above matrix is of rank of 3 and hence there are a maximum of three independent constraints on the $\bar{c_i}$. For the new six-noded triangles with curved sides used in axisymmetric conditions, the three-point integration rule implies that for limiting case of a very fine mesh the number of degree of freedom per constraint is equal to $\frac{4}{3}$. It is interesting to note that if a higher order quadrature scheme is used, for example a six-point rule, then the left hand side of equation (87) will have rank six, which tends to increase the number of constraints per element from three to six.

In summary, it is suggested that the new six-noded triangle is not only suitable for use in axisymmetric grids where all the element sides are straight, but also satisfactory for use in axisymmetric configurations where all triangles sides are curved provided a three-point rule is used. It has been shown that a three-point rule used in the new six-noded triangles under axisymmetric loading is able to assess the elastic strain energy correctly. It was also noted that a six-point rule used for the new six-noded triangles with curved sides implies that the limiting number of degree-of-freedom per constraint is equal to $\frac{4}{6}$, which is not satisfactory. Note, however, that for axisymmetric problems in which only a few of the elements have curved sides, the new six-noded triangular element when using with a six-point integration rule is likely to be satisfactory. This is because analysis performed in this section gives an upper bound on the overall number of constraints as it has been assumed that all element sides are curved. The same argument can be applied to the suitablity of the conventional six-noded triangular elements used in plane strain grids where all the element sides are curved.

NUMERICAL EXAMPLES

In the preceding section, a theoretical proof of the new displacement interpolation function and two alternative finite element formulations using the proposed velocity expansion were presented. This section is devoted to a description of the numerical verification of the proposed formulations. Although many examples exist for this purpose, attention is focused on the prediction of stress distribution for small strain thick cylinder expansion and collapse load for a circular footing problem. This is intended to assess numerically the suitability of the proposed formulations used for axisymmetric problems of nearly incompressible materials. The detailed numerical procedure, which can be found in *Yu*[12], will not be repeated here.

A Small Strain Thick Cylinder Expansion in a Elastic Incompressible Material

In order to investigate the effects of incompressibility on the quality of stress data calculated using the displacement finite element formulation presented in this paper, the analysis of a small strain thick cylinder problem was carried out . The problem consisted of a thick-walled cylinder, with inner radius a and outer radius b, subjected to an internal pressure P. To isolate possible errors due to the non-linear solution algorithm, a material with infinite strength has been assumed so as to ensure a purely linear elastic response. The expansion of an infintely long cylinder was modelled by prescribing a plane strain condition in the vertical direction. The mesh used for calculation is shown in Figure 5. A Poisson's ratio of 0.49 was used to approximate incompressible material behaviour. The expansion of a cylinder was carried out by applying a radial pressure along the inner boundary of the cylinder.

The computed stresses were normalised by the applied internal pressure P and plotted in Figure 5. The analytical solutions by *Hill*[13] are also shown in the same diagram. It is found that the finite element results approximate closely the exact solutions for the perfectly incompressible case.

A Smooth Rigid Circular Footing On a Deep Purely Cohesive Undrained Layer

This problem is selected to assess numerically the suitablity of the proposed formulations used for plastic analysis of nearly incompresibble materials. In the calculation presented in this section, the mesh shown in Figure 6 has been used. The semi-infinite soil mass is modelled by a square mesh with each side equal to 10B, where B is the radius of the footing. Around the edge of the footing, a refined mesh system is used correctly to model the high stress gradients and failure mechanism. Note the slightly curved element edges, since they are straight in the generalized (R, z) space.

A collapse load calculation for a smooth footing resting on weightless von Mises soils has been performed. In the calculation, a uniform vertical displacement was prescribed to the footing base and horizontal movement of the nodes in contact with the footing was left free to simulate a smooth footing. The resulting load displacement curve is plotted in Figure 7. For a perfectly plastic von Mises material, no exact collapse load is known. However the collapse load must be greater than the solution obtained for a Tresca material (*Shield*[14]) and less than the solution for the Tresca material multiplied by a factor of $\frac{2}{\sqrt{3}}$. This is because in triaxial stress states the von Mises yield surface is equivalent to the Tresca yield surface and in plane strain conditions the von Mises yield surface represents the Tresca surface scaled by a factor of $\frac{2}{\sqrt{3}}$. The stress state created by loading a circular footing corresponds neither to a triaxial stress state nor plane strain conditions. As shown in Figure 7, the finite element analysis yields a well defined collapse load which is between these two collapse loads for triaxial stress states and plane strain conditions. The result shown in Figure 7 supports the statement that the new six-noded triangular element will be able to capture the true limit load accurately for axisymmetric problems of nearly incompressible materials, provided a sufficiently fine mesh is used.

CONCLUSIONS

The theoretical criterion originally developed by *Nagtegaal et al*[1] has been used to assess the suitability of a particular displacement interpolation function when it is used together with any constitutive model which requires that the constant volume condition is enforced. A six-noded triangle with a novel velocity expansion was found to be able to satisfy the criterion under axisymmetric configurations.

Based on the proposed displacement interpolation function, two alternative isoparametric finite element formulations have been developed using the virtual work principle. The finite element formulation based on the modified shape function matrix can be easily implemented into any existing displacement-based finite element program with minor changes to the strain rate -nodal velocity matrices in a traditional stiffness formulation. By contrast, the proposed formulation based on the modified basic variables requires slightly more modifications in a conventional displacemnt formulation.

The results of the numerical analyses of both elastic and plastic incompressible behaviour confirm the theoretical predictions. For the analysis of a circular footing resting on a nearly incompressible material, the new six-noded triangular element was found to be capable of predicting a well defined collapse load.

Although a rigorous extension of the theoretical proof of the proposed formulations to a dilational material has not been presented, the results for a circular footing resting on a frictional material with the Matsuoka plasticity model presented by Yu^{12} suggest that the proposed formulations are also able to capture the limit load within a reasonable bound for axisymmetric analyses of dilational materials, provided a sufficiently fine mesh is employed.

The proposed formulations described in this paper have been developed on the assumption that strains and displacements are small. The generalization of the formulations to problems of large elastic-plastic deformation has already been carried out by Yu^{12}. However, full discussion of these extended formulations is beyond the scope of this paper.

ACKNOLEDGEMENTS

The work presented in this paper was carried out while the first author was a research student at University of Oxford. The authors wish to thank Dr Scott Sloan of the University of Newcastle, Australia for his useful and stimulating discussions with the authors about the use of finite element methods in the analysis of incompressible materials.

REFERENCES

1. J.C. Nagtegaal, D.M. Parks and J.R. Rice,'On numerically accurate finite element solutions in the fully plastic range', *Comp. Meth. Appl. Mech. Eng.*, **4**,153-177(1974).

2. S.W. Sloan,'Numerical analysis of incompressible and plastic solids using finite elements', Ph.D. Thesis, University of Cambridge, 1981.

3. S.W. Sloan and M.F. Randolph,'Numerical prediction of collapse loads using finite element methods', *Int. J. Num. Anal. Meth. Geomech.*, **6**, 47-76(1982).

4. H.S. Yu and G.T. Houlsby,'A new finite element formulation for one dimensional analysis of elastic-plastic materials', *Computers and Geotechnics*, **9**, 242-256(1990).

5. D.J. Naylor,'Stresses in nearly incompressible materials by finite elements with application to the calculation of excess pore pressures', *Int. J. Num. Meth. Eng.*, **8**, 443-460(1974).

6. H.J. Burd and G.T. Houlsby,'Finite element analysis of two cylindrical cavity expansion problems involving near incompressible material behavior', *Int. J. Num. Anal. Geomech.*, **14**, 351-366(1990).

7. C.T. Toh and S.W. Sloan,'Finite element analyses of istropic and anisotropic cohesive soils with a view to correctly predicting collapse', *Int. J. Num. Anal. Meth. Geomech.*, **4**, 1-23(1980).

8. O.C. Zienkiewicz, R.L. Taylor and T.M. Too,'Reduced integration technique in general analysis of plates and shells', *Int. J. Num. Meth. Eng.*, **3**, 275-290(1971).

9. D.S. Malkus and T.J.R. Hughes,'Mixed finite element methods - reduced and selective integration techniques: a unification of concepts', *Comp. Meth. Appl. Mech. Eng.*, **15**, 63-81(1978).

10. R. de Borst and P.A. Vermeer,'Possibilities and limitations of finite elements for limit analysis', *Geotechnique*, **34**, 199-210(1984).

11. M.E. Laursen and M. Gellert,'Some criteria for numerically integrated matrices and quadrature formulas for triangles', *Int. J. Num. Meth. Eng*, **12**, 67-76(1978).

12. H.S. Yu, 'Cavity expansion theory and its application to the analysis of pressuremeters', DPhil Thesis, University of Oxford, England, 1990.

13. R. Hill, 'The mathematical theory of plasticity', Oxford University Press, 1950.

14. R.T. Shield,'On the plastic flow of metals under conditions of axial symmetry', *Proc. Roy. Soc.*, London, **A.233**, 267(1955).

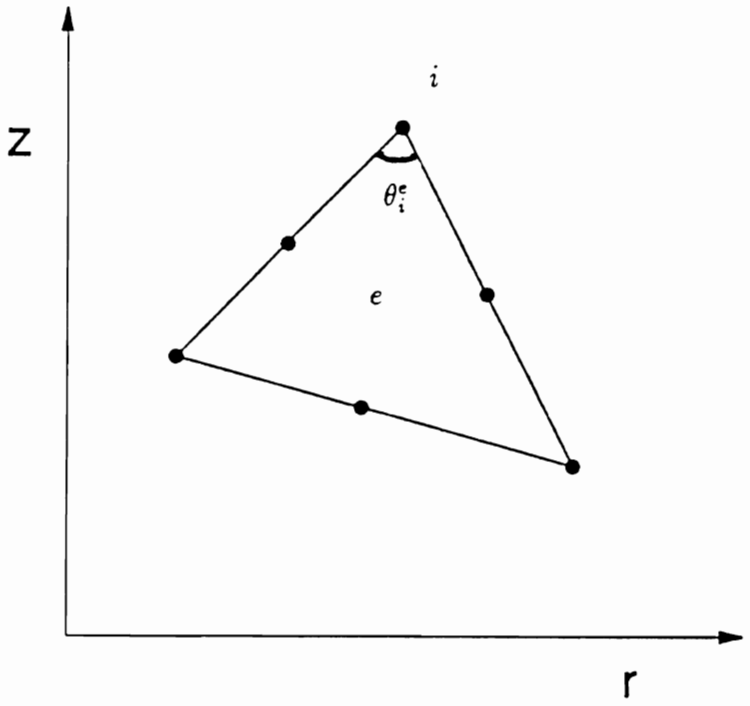

Figure 1: A six-noded triangle element

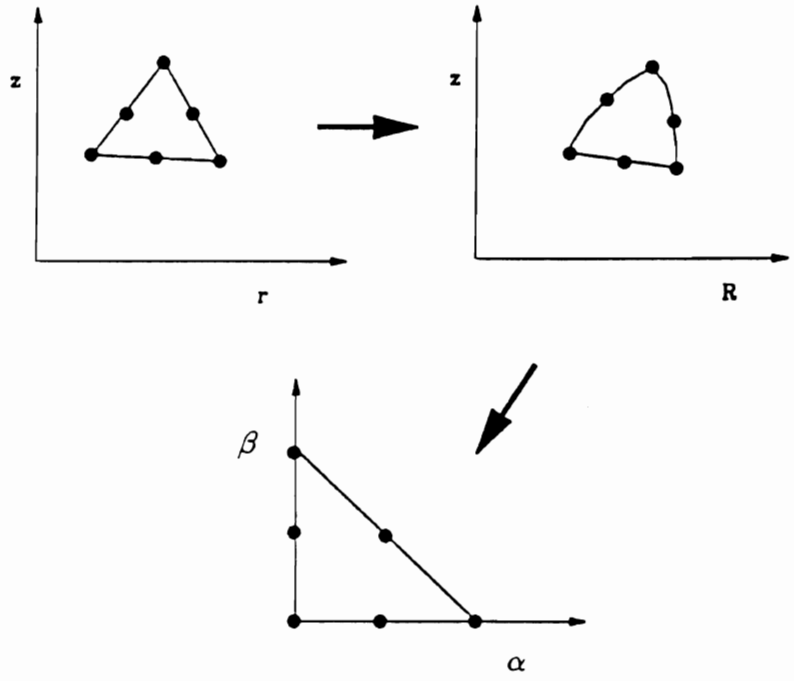

Figure 2: Mapping of an isoparametric six-noded triangular element

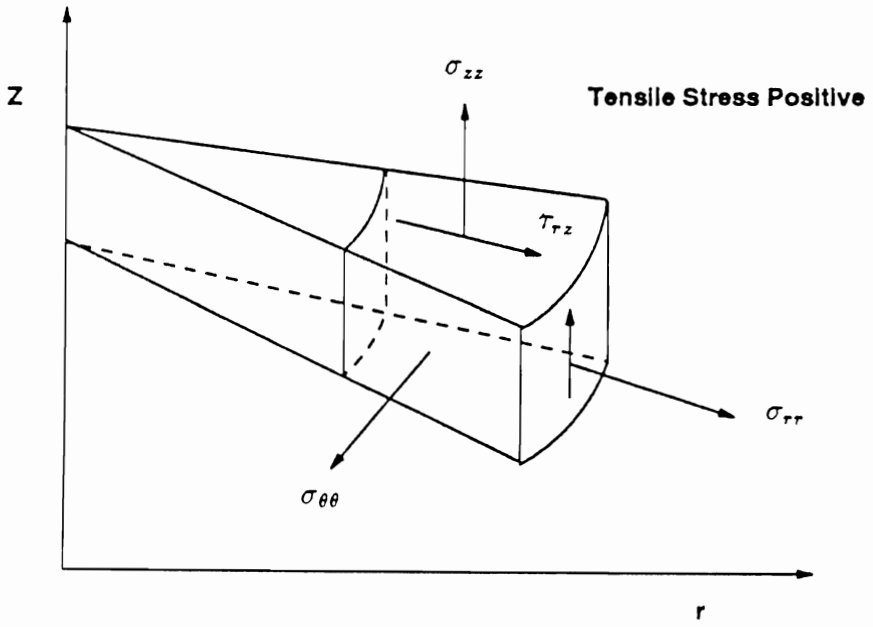

Figure 3: Definition of stresses in axisymmetric geometry

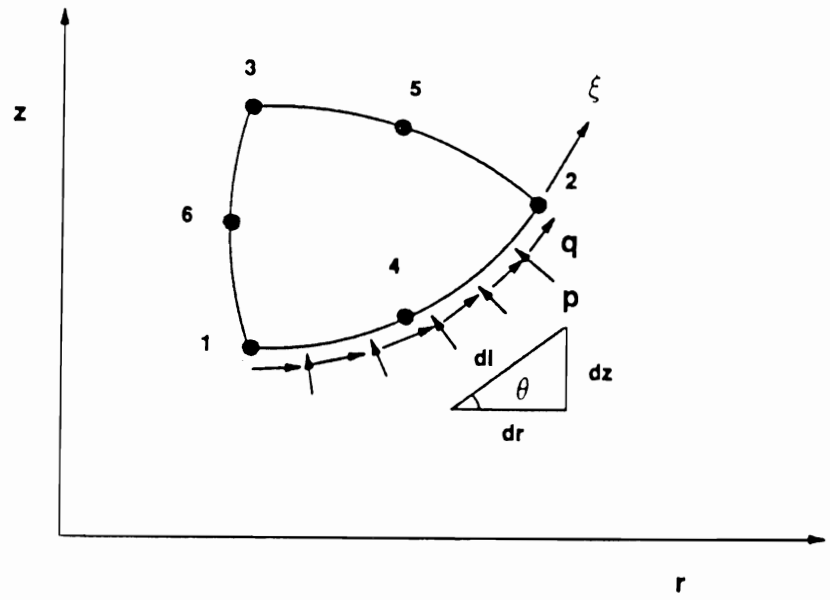

Figure 4: Calculation of distributed surface loadings

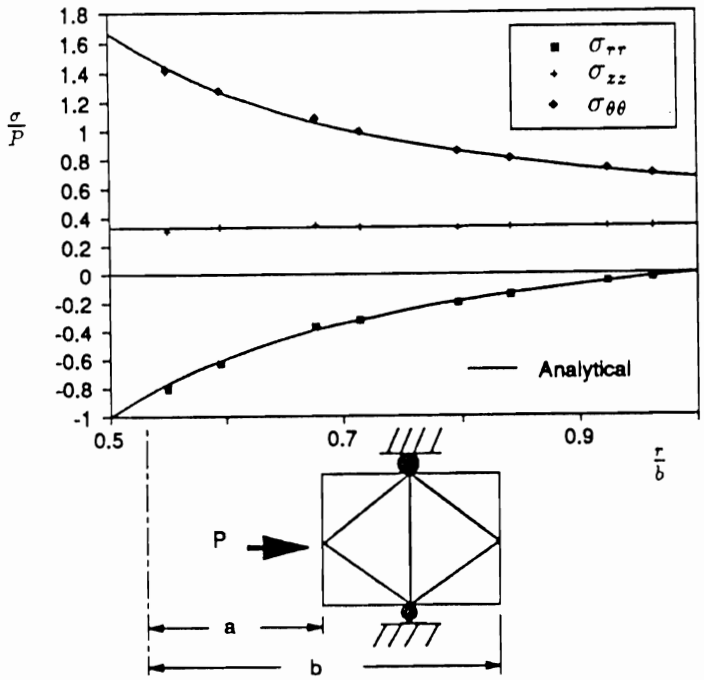

Figure 5: Finite element mesh and results for cylinder expansion

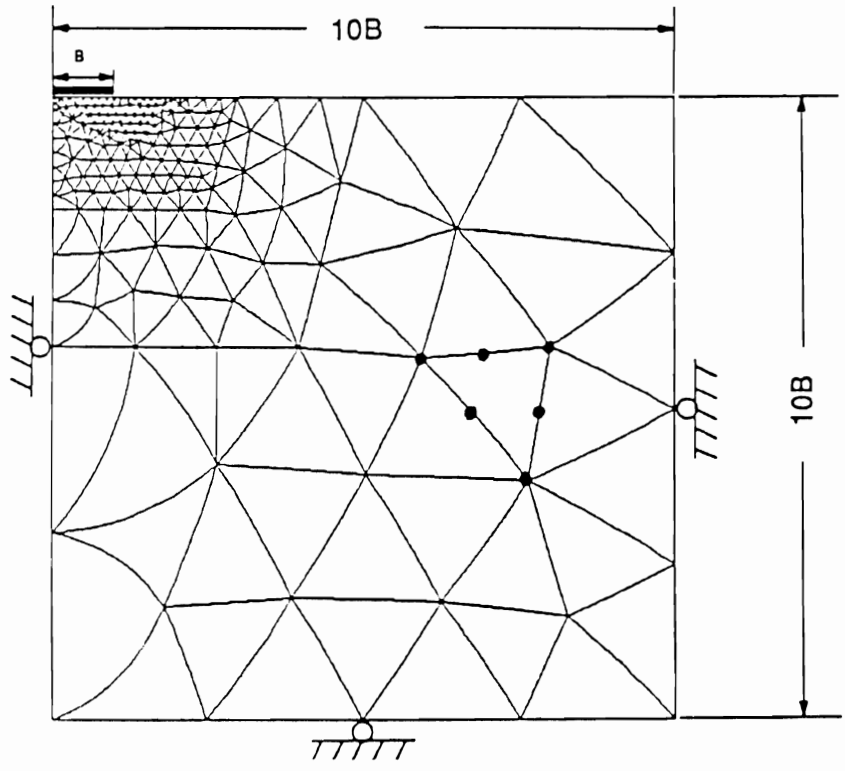

Figure 6: Finite element mesh for collapse load calculation

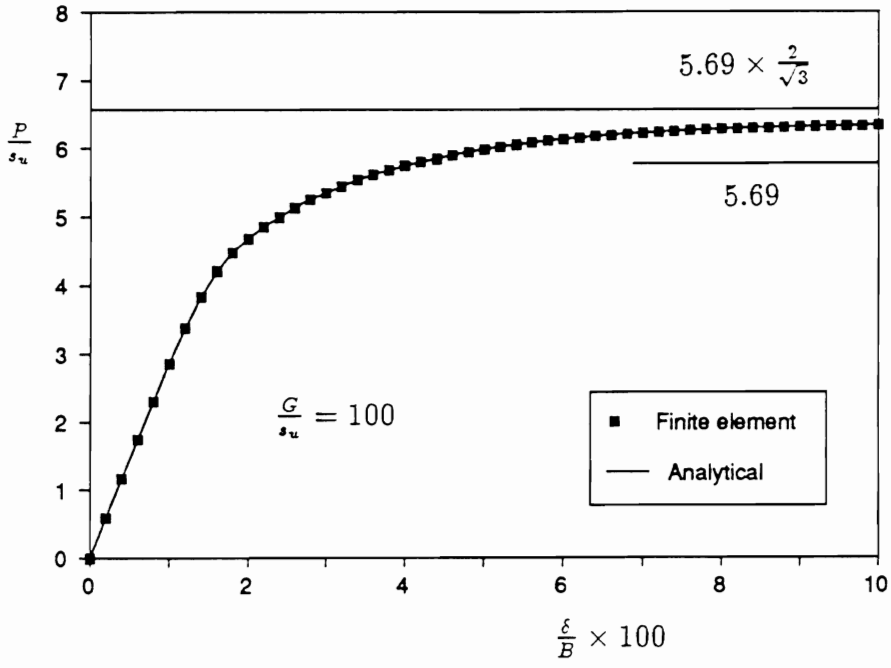

Figure 7: Numerical footing pressure-displacement curve